Canted states in anti-ferromagnetically coupled magnetic bilayers

External traineeship report

Canted states in anti-ferromagnetically coupled magnetic bilayers

Author:
Fanny Ummelen

Supervisor:
Dr. Amalio
Fernández-Pacheco

August 2013

Abstract

Bilayer systems of ultra-thin anti-ferromagnetically coupled Co and CoFeB layers have been systematically investigated. The intention was to find systems in which the magnetization of one of the layers (or both) would be in a canted state, meaning that the magnetization is neither in-plane nor out-of-plane at remanence. We have indeed been successful in obtaining such systems, observing configurations where one layer is out-of-plane and one is canted, and others where one layer is in-plane and one is canted. In this work we will discuss other phenomena that have been observed, such as the presence of an in-plane bias field or the competition between the switching fields of both layers as a function of the sweeping field rate.

Contents

Chapter 1

Introduction

Magnetic thin layers normally have a magnetization that is either in-plane or out-of-plane at remanence. However, it would be interesting for some applications if the magnetization could be something in between, forming a canted state. Applications would include more efficient switching of MRAMs using spin transfer torque [1] [2] or inserting data in a three dimensional computer memory [3]. Canted states have been observed in literature [4] [5] [6]. However, most cases only epitaxial films are investigated. In this study canted states are pursued in films produced by sputtering.

Chapter 2

Theory

2.1 Canted states and their applications

Thin films of magnetic materials usually have an in-plane or out-of-plane anisotropy, depending on the thickness and interactions at the surface. Suppose that the magnetization is neither in-plane nor out-of-plane at remanence, than it is called a canted state. Two possible applications of canted states are discussed in this section.

2.1.1 The soliton stack

Imagine a stack of thin magnetic layers with an out-of-plane anisotropy that are antiferromagnetically coupled. The ground state of this system would have layers with alternating up or down magnetization in the stack. If two adjacent layers had the same magnetization, both up or both down, this would be a frustration in the system, called a magnetic kink soliton. It has been shown that these systems can be grown, and that a soliton can be inserted, measured and propagated [3]. The idea is to build a three dimensional computer memory out of these soliton stacks in the future. However, for this application it would be required to inject multiple solitons in one stack, which requires a more robust soliton injection mechanism than the one currently used. Canted states might offer the solution. For the design of a soliton insertion mechanism the switching fields of the the individual layers in the stack is of major importance. In a canted state it would be potentially possible to bias the switching field in the out-of-plane direction with fields in the in-plane direction. This would give another parameter to design a better soliton insertion mechanism.

2.1.2 MRAM

Magnetoresistive random-access memory, MRAM, is a novel way to store data. Information is stored in magnetic layers with an insulting layer between them. A current can tunnel through this insulting barrier. The resistance of this barrier is dependent on the magnetization of the magnetic layers; if the layers have a parallel magnetization the tunneling is easy and the resistance is low, if the layers have an anti-parallel magnetization the tunneling is difficult and the resistance is high. This way a "zero" or a "one" can be defined. The conventional way to switch the layers is using magnetic fields, but scaling down in power consumption and size is problematic when this method is used. Another way of switching the layers which does not have this disadvantage is the use of spin transfer torque, STT. In this case one of the layers has a fixed magnetization which polarizes the current when it flows through it. The electrons transfer a torque on the other layer which can be switched. The problem with this method is that the current densities needed for switching are too high. One issue is that the transferred torque is proportional to the sine of the the angle between the magnetization of the layer, $STT \propto \sin\theta$, and is only non-zero in practise due to thermal fluctuations. If one of the layers would be in a canted state this alignment would not be perfect and the spin transfer torque would be larger, making the switch easier [1] [2].

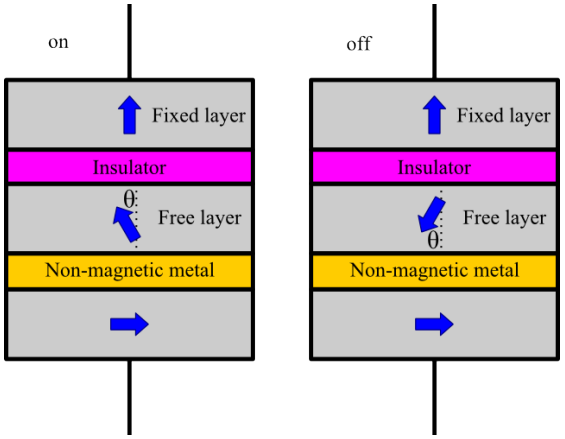

FIGURE 2.1: Schematic representation of two elements of an MRAM device, one in the on and one in the off state, both with one layer in a canted state.

2.2 The studied systems

In this study we try to produce canted states using the motif shown in figure 2.2. The bottom layer of Tantalum, Ta, provides a smooth surface for the layers that follow. The top Ta protects the sample from oxidation. The Cobalt, Co, and Cobalt-Iron-Boron, CoFeB, are the magnetic layers. Two different material are chosen because they have a

different magnetic hardness, which gives more possibilities. The magnetization of these layers will be indicated with arrows throughout this report, an example of this is given in figure 2.2. The white arrow represents Co, the blue arrow represents CoFeB. The Ruthenium, Ru, layer provides the non-magnetic layer to create RKKY coupling. The Platinum, Pt, layers favor an out-of-plane magnetization for the magnetic layers, and varying their thickness is a way to vary the strength of the RKKY coupling [7].

In the right part of figure 2.2 a schematic sample with a coordinate system attached to it is depicted. The definition of the axes in this picture will be used in the remainder of this report; the z direction is perpendicular to the surface of the sample, the x and y directions are in the plane of the surface of the sample.

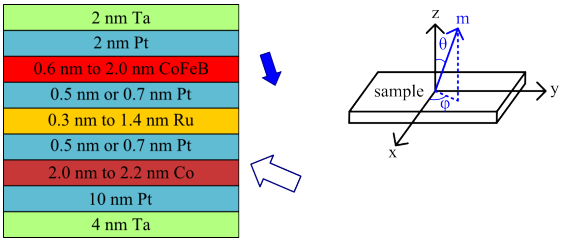

FIGURE 2.2: Schematic representation of the samples that will be studied in this report.

Most studies on bilayers are on systems that have both magnetic layers in-plane or both magnetic layers out-of-plane at remanence, systems with a canted state at remanence are quite rare. In this study it is tried to grow canted states by making one in-plane layer and one out-of-plane layer, one of them close to the spin reorientation transition. Due to the coupling this could result in a canted state. To find the parameters that result in a canted state the thicknesses of the layers are varied in steps of one Ångström, which is an experimental challenge.

2.3 Basic theory

In previous sections it was mentioned a few times that the magnetization of a magnetic layer can be in-plane, out-of-plane or canted. What configuration is energetically favorable depends on the anisotropy and coupling between layers. These effects will be briefly discussed in this section.

2.3.1 Anisotropy

Anisotropy is plays a central role in this project. Basically it means that the magnetization prefers certain directions over others. In general, when the magnetization is along a

random direction in space, and considering in-plane and out-of-plane anisotropies, this is described by equation 2.1, where the different K are the anisotropy constants. The angles and directions are defined in figure 2.3.

$$E = K_{1eff} \sin^2\theta + K_2 \sin^4\theta + ... + K_v \frac{|\vec{m} \times \hat{x}|^2}{|\vec{m}|^2} \tag{2.1}$$

K_{1eff} actually consists of two terms:

$$K_{1eff} = \frac{2K_S}{t} - 2\pi M_S^2 \tag{2.2}$$

The first term a crystalline anisotropy term. The physical origin of the term is spin orbit coupling at the surface of the magnetic film, which favors an out-of-plane anisotropy. The platinum at the surface of our magnetic layers enhances this effect. Because this is a surface effect it will become less important for thicker layers.

The second term in equation 2.2 is the demagnetization term. It can be understood in the following way: a magnetic body can be thought of as consisting of a lot of small magnets. If the magnetization is uniform, the poles of the small magnets will be compensated inside the body but free magnetic poles will exist on the surface. The distance between the poles and the density of the poles on the surface now depends on the direction of the magnetization if the body is not spherical. In general it is energetically more favorable to align the magnetization along the longest axis of the body. In a thin film this means that an in-plane magnetization is more favorable than an out-of-plane magnetization. Note that this term depends solely on the shape of the magnetic material, not on the crystal structure. From the sign of K_{1eff} it can be seen whether it is more favorable for the magnetization to be in-plane or out-of-plane.

The term in 2.1 starting with K_2 is the second order anisotropy term. Third, fourth etc. order anisotropy terms exist as well, but are neglected here. In fact, K_2 is normally neglected as well. Around the spin reorientation transition, the thickness for which the system passes from out-of-plane to in-plane, K_{1eff} is equal to zero. Around this point K_2 is not negligible anymore [8].

The last term in equation 2.1 describes a preferential direction in the plane. In this case the magnetization along the x direction is more favorable than along the y direction. In the cases considered here, this term is much smaller than the first term.

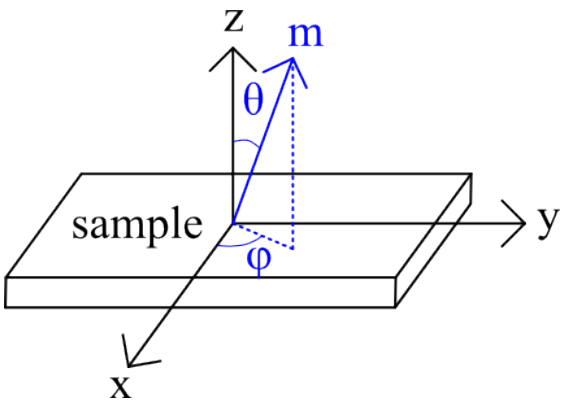

FIGURE 2.3: Definition of the directions and angles used in this report.

2.3.2 RKKY coupling

When a thin film of non magnetic metal is sandwiched between two films of magnetic material, the magnetic materials get coupled. Whether this is ferromagnetic (the magnetization of the two layers align parallel to eachother) or anti-ferromagnetic (the magnetization of the two layers align in opposite directions) depends on the thickness of the non magnetic spacer. This effect can be described by the Ruderman-Kittel-Kasuya-Yosida, or RKKY, model. An indirect exchange coupling between the electrons in the magnetic layers can exist via the conduction electrons in the non-magnetic one. Details can be found in literature [9].

The strength of the coupling between magnetic layers can be quantified with the energy per unit area J. The coupling field experienced by a layer can be calculated using equation 2.3.

$$H_J = \frac{J}{M_S t} \tag{2.3}$$

In this equation M_s the saturation magnetization and t the thickness of the layer, all in cgs units.

Chapter 3

Experimental Techniques

3.1 Production of the samples

All samples discussed in this report are prepared using sputtering. A silicon substrate of approximately 1 cm^2 is mounted on a sample holder and loaded into a vacuum chamber. The vacuum chamber used reaches pressures between 0.3×10^{-7} and 1.0×10^{-7} bar. In the chamber several targets of different material are present, in our case platinum, ruthenium, cobalt, cobalt-iron-boron, aluminium and tantalum. Argon gas is inserted into the chamber and a plasma is ignited on one of the targets. High energetic atoms are released from the target, hit the substrate and stick to it. The samples holder spins around during this process, to achieve uniform growth. This way layers can be grown with Ångström precision in their thickness. Figure 3.1 shows a schematic picture and figure 3.2 a photograph of the setup.

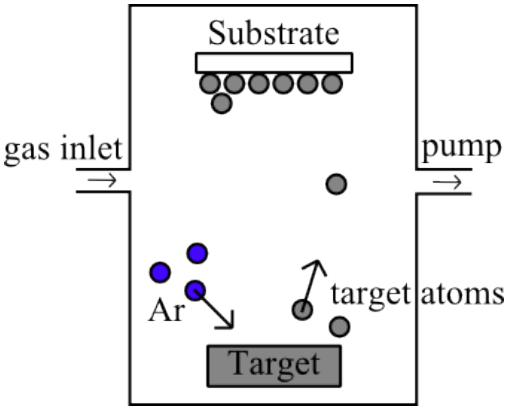

FIGURE 3.1: Schematic setup of the sputter machine.

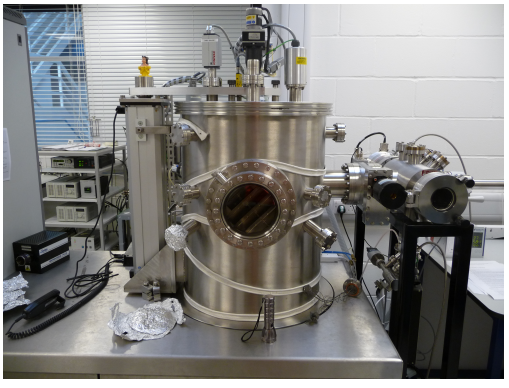

FIGURE 3.2: Photograph of the used sputtering machine.

3.2 Characterization methods

We are interested in the magnetic properties of the grown samples. The magnetization can be measured using two methods: magneto-optic Kerr effect, MOKE, or vibrating sample magnetometer, VSM. MOKE measurements are fast and measure only a small spot on the surface. VSM is slow and measures contributions to the magnetization from the entire sample. Both methods will be used to characterize the samples, so both techniques are discussed in this chapter.

3.2.1 MOKE

MOKE stands for magneto-optic Kerr effect. It refers to the phenomenon that light changes its polarization when it is reflected from a magnetic surface. This effect can be experimentally measured using a Kerr microscope, for which the schematic setup is shown in figure 3.3. The change in polarization is a measure for the magnetization of the material where the light is reflected of.

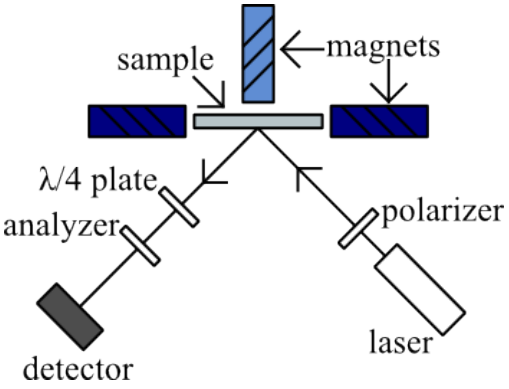

FIGURE 3.3: Schematic setup for MOKE measurements.

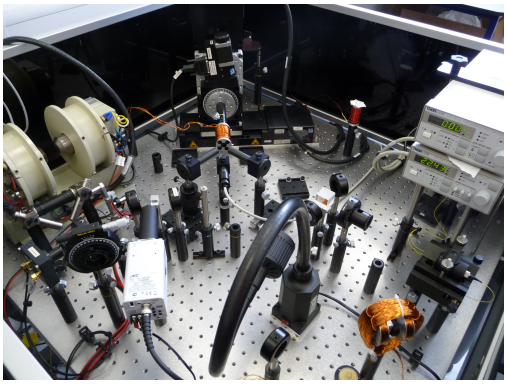

FIGURE 3.4: Photograph of one of the used MOKE setups.

First the laser light passes through a polarizer to polarize the light. Then the light is reflected of the sample that is investigated and the Kerr effect occurs. The light passes through an analyzer which makes the intensity a measure for the magnitude of the Kerr effect, measured by the detector. A quarter lambda plate can be added to measure the change in ellipticity instead of the change in rotation. Magnetic fields can be applied to the sample during the measurement to obtain hysteresis loops. For in-plane measurements the dark blue magnets are used, for out-of-plane measurements the light blue magnet is used, see figure 3.3. The polarization of the light can be changed by a magnetization component perpendicular to the plane of the sample, polar MOKE, or a magnetization component in the plane of the sample and in the plane of

incidence, longitudinal MOKE, which in case of materials with canted states, can make the interpretation of data difficult.

Three different MOKE setups are used during this study. The first setup is shown in figure 3.4 and is used for both in-plane and out-of-plane measurements and both rotational and elliptical Kerr measurements. In the second setup the angle between the incoming and reflected laser beam is very small, making sure that only the polar Kerr effect is measured. The last setup has a 5 μm laser spot that rasters the surface to form a magnetic image of the sample. This setup is used to image the domains during switching of the magnetization. In this setup the angle between the incoming and reflected beam is very small as well, so again only the polar Kerr effect is measured.

3.2.2 VSM

A vibrating sample magnetometer or VSM, is an experimental instrument based on Faraday's law, a magnetic field changing in time induces an electric field.

$$\nabla \times E = \frac{\partial B}{\partial t} \tag{3.1}$$

A magnetic sample is mounted on a sample holder and is vibrated in the y-direction between the pickup coils. This induces a voltage in the coils which is a measure for the magnetization of the sample, and can be measured using a lock-in amplifier. An external magnetic field can be applied, so a hysteresis curve of the sample can be measured. The magnetic fields can be applied perpendicular to the plane of the sample (z direction) or along the plane of the sample (x direction) depending on how the sample is mounted, see figure 3.5. Because two sets of pick up coils are available, both the out-of-plane component as one of the in-plane components of the magnetization can be measured simultaneously.

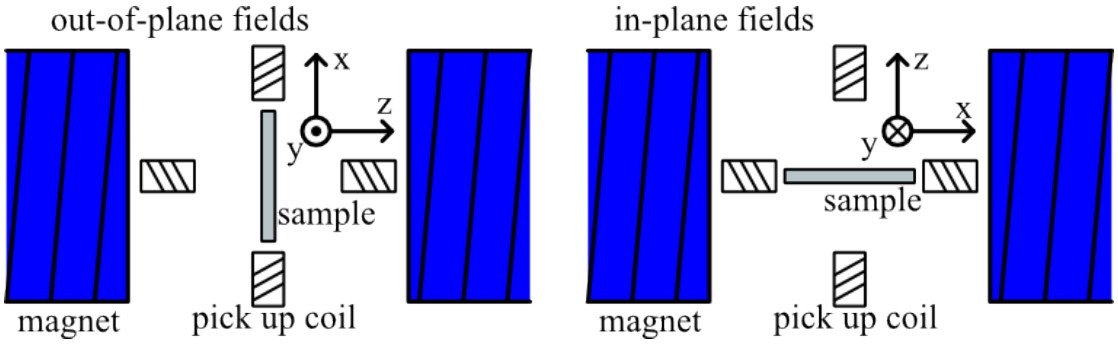

FIGURE 3.5: Top view of a schematic setup for VSM measurements.

3.2.3 simulations

The studied systems are also investigated theoretically using simulations. Experimental results will be reproduced by the simulations which should give insight in the physics and make it possible to deduce the behavior of the magnetization of the individual layers. Two different programs are used. Both programs use the macrospin approximation; so one layer behaves like one big spin, domains cannot exist. The first program uses an Ising model, the magnetization of a layer can be up or down, nothing in between. This program is suitable for simulating systems with a high K_{1eff}, because for these systems the Ising model is a good approximation. The other program is a non-Ising Monte Carlo code, the spins can rotate gradually. This is necessary to simulate a canted state.

Chapter 4

Results and Discussion

4.1 Tools for understanding bilayer systems

The final goal of this project is to couple a magnetic layer with in-plane anisotropy to a layer with out-of-plane anisotropy, which could result in a canted state. However, simpler systems have to be investigated first in order to make it possible to understand these complicated bilayers. An investigation of single layers is done first to teach us when we should expect a layer to have an in-plane or out-of-plane anisotropy. Then bilayers are grown with parameters for which we are certain that both layers are in-plane or out-of-plane.

4.1.1 The spin reorientation transition in cobalt

A series of single Co layers of different thicknesses, varying from 0.6 nm up to 2.2 nm, is grown and analyzed using MOKE. These measurements allow us to see for which thicknesses Co has an in-plane or an out-of-plane anisotropy and at which thickness the spin reorientation transition occurs. The results are shown in figure 4.1 to 4.4.

For thicknesses between 0.6 nm and 0.9 nm the loops are all similar; the transition from negative to positive magnetization and vice versa, is sharp and occurs at coercive fields of about 500 Oe, see figure 4.1. For higher thicknesses, up to 1.7 nm the transitions stay sharp, but the coercive fields gradually decrease, see figure 4.4. For the 1.8 and 1.9 nm thick samples the behavior is different; the transitions are clearly more slanted, see figure 4.2. Then between 1.9 and 2.0 nm the spin reorientation transition occurs, because from 2.0 nm on the system shows in-plane behavior, see figure 4.3. It seems that there still is some out-of-plane coercivity, but this may be an artifact from the MOKE measurements or it could be a mixture of the longitudinal and polar Kerr effect. Also

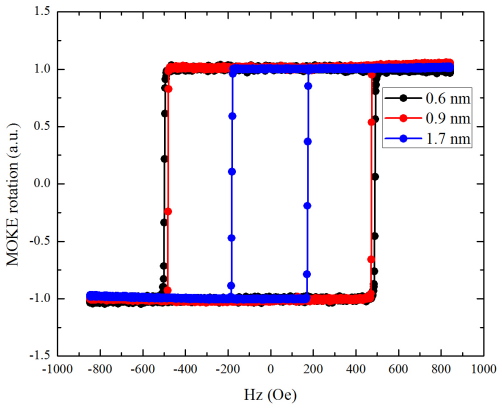

FIGURE 4.1: Hysteresis loops of single layer samples before the spin reorientation transition.

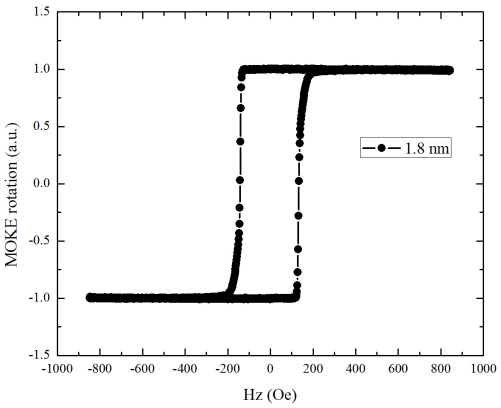

FIGURE 4.2: Hysteresis loop of a single layer sample close to the spin reorientation transition.

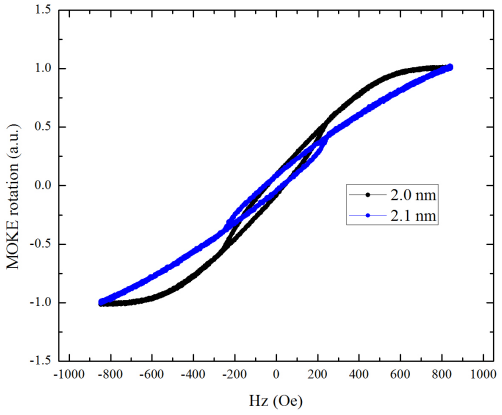

FIGURE 4.3: Hysteresis loops of single layer samples after the spin reorientation transition.

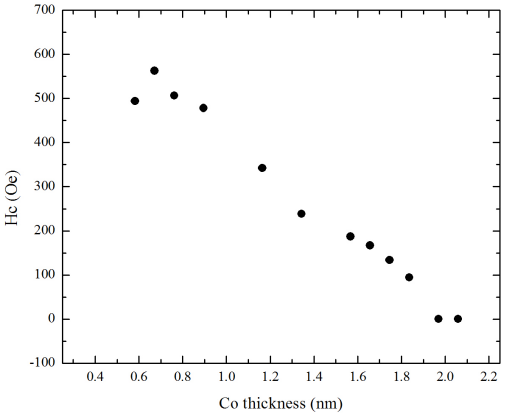

FIGURE 4.4: The coercive fields of single layers as a function of their thickness at a sweep rate of 17000 Oe/s.

it can be seen that the slope of the graph decreases when the thicknesses is increased from 2.0 to 2.2 nm, indicating that it becomes more difficult to pull the magnetization out-of-plane. Finally, for samples thicker than 2.2 nm (not shown here) saturation is not reached anymore using the maximum field applied, of 900 Oe. This is qualitatively in agreement with [10], though a different value for the thickness of the spin reorientation transition is found in this article.

In theory it should be be possible to find a canted state in this series when very small steps in thickness are taken around the spin reorientation transition. In section 2.3.1 the equation for the energy is given. The spin reorientation transition is very sharp when K_2 is negligible; it happens exactly when K_{1eff} changes from positive to negative. However, in reality K_2 is unequal to zero, and becomes of importance around the spin reorientation transition when K_{1eff} becomes small. In literature [11] it has been shown that this can result in a canted state when $K_2 > -0.5K_{1eff}$. This happens in a very small range of thicknesses and is difficult to control. Therefore the goal of this report is

to produce canted states using coupling between two layers with competing anisotropy directions and not using single layers.

The spin reorientation transition is measured to occur between 1.9 nm and 2.0 nm. The saturation magnetization of Co is known to be 1400 emu/cm^3. From this K_S can be calculated to be 1.2 erg/cm^2. The spin reorientation transition in CoFeB layers was measured before by Dr. A. Fernández-Pacheco and occurs at 1.6 nm. This together with a measured CoFeB saturation magnetization of 1200 emu/cm^3 gives $K_S = 0.7$ erg/cm^2. These values for K_S are used in all simulations presented in this report.

The switching of the magnetization is also investigated using MOKE imaging, the results are shown in figure 4.5 to 4.8. For layers of 1.6 nm or thinner the switching happens through big domains (see figure 4.5). When the thickness becomes closer to the spin reorientation transition the domains become smaller and the transition becomes more nucleation dominated, see figure 4.6 to 4.8. This can be understood following energy arguments, and is in agreement with what is found in literature [12] [10].

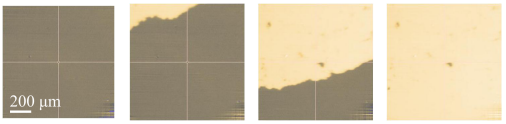

FIGURE 4.5: Polar MOKE images of a 1.6 nm Co layer during switching.

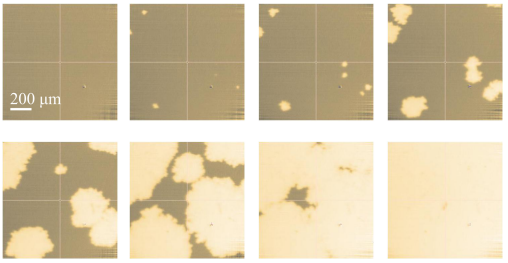

FIGURE 4.6: Polar MOKE images of a 1.7 nm Co layer during switching.

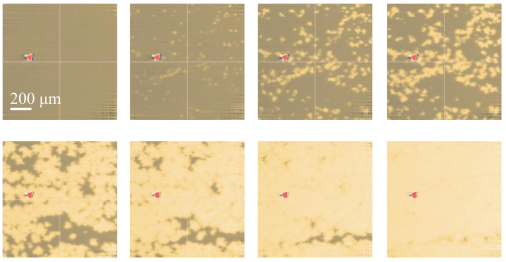

FIGURE 4.7: Polar MOKE images of a 1.8 nm Co layer during switching.

FIGURE 4.8: Polar MOKE images of a 2.0 nm Co layer during switching.

4.1.2 The extreme cases; everything in-plane or everything out-of-plane

Bilayer samples are grown with thicknesses for which it is certain they are either in-plane or out-of-plane. This is done for two different Pt spacer thicknesses. A thicker Pt spacer corresponds to a weaker coupling between the layers [7]. Along this report

"strong coupling" refers to systems with 0.5 nm thick Pt spacers and "weak coupling" to systems with 0.7 nm thick Pt spacers. The results are shown in figures 4.9 to 4.12.

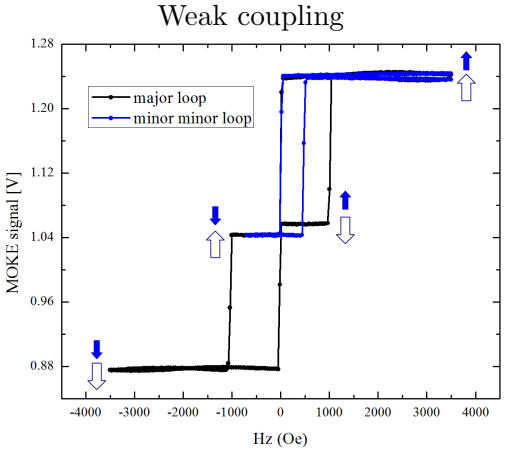

FIGURE 4.9: Out-of-plane MOKE measurement of two weakly coupled layers with out-of-plane anisotropy.

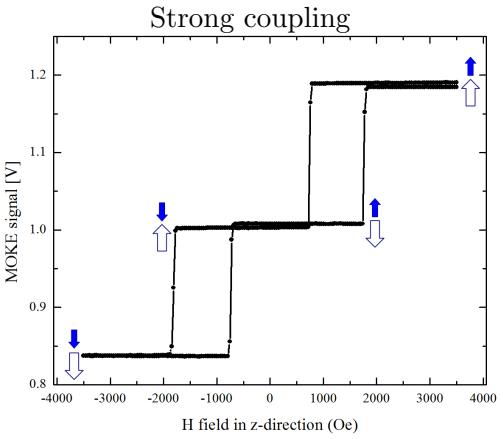

FIGURE 4.10: Out-of-plane MOKE measurement of a two strongly coupled layers with out-of-plane anisotropy.

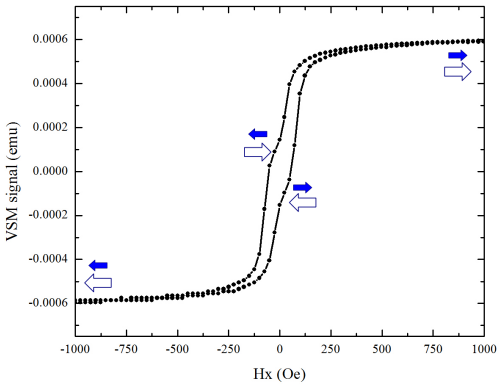

FIGURE 4.11: In-plane VSM measurement of two weakly coupled layers with in-plane anisotropy.

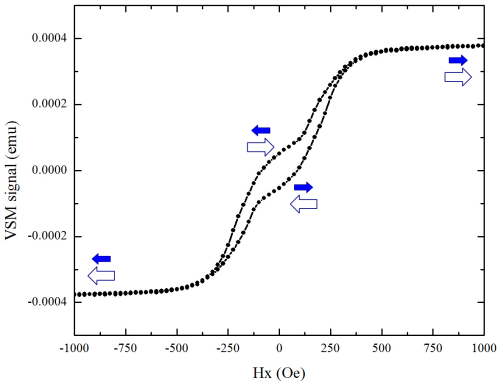

FIGURE 4.12: In-plane VSM measurement of a two strongly coupled layers with in-plane anisotropy.

In the out-of-plane samples the coupling is determined from the minor loops; the transitions occur at $H_J - H_C$ and $H_J + H_C$ respectively. The in-plane samples show a spin-flop behavior. The coupling can be determined from the saturation magnetic field, though due to the curvature of the graphs, this cannot be done very precise.

The systems are also simulated. The results for the systems with strong coupling are shown in figure 4.13 and 4.14. The out-of-plane case can be reproduced perfectly using the macrospin Ising model previously described, indicating that the system behaves as an Ising system. The in-plane system can also be reproduced quite well using the non-Ising software. Note that the plateaus where the magnetization is antiparallel are not very flat in the experiment, though they should be according to the simulations. This is because the VSM picks up signal from the entire sample, and some areas, especially those close to

the edge of the sample, may behave a bit differently, while in the simulations everything is ideal. What can be learned from the simulations is that the in-plane anisotropies are very low and that the Kv for Co is relatively high in comparison with the Kv for CoFeB. This could be because the in-plane preferential direction is induced by the substrate, and the the Co layer is deposited before the CoFeB layer.

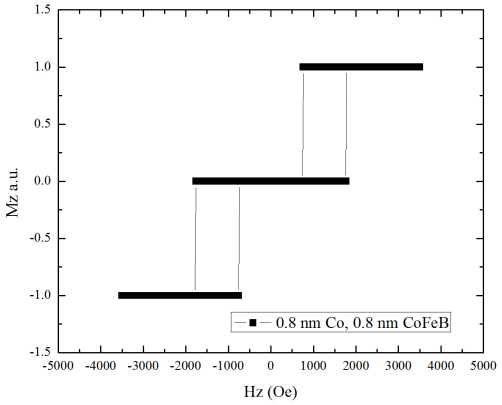

FIGURE 4.13: Simulation of two strongly coupled out-of-plane layers.

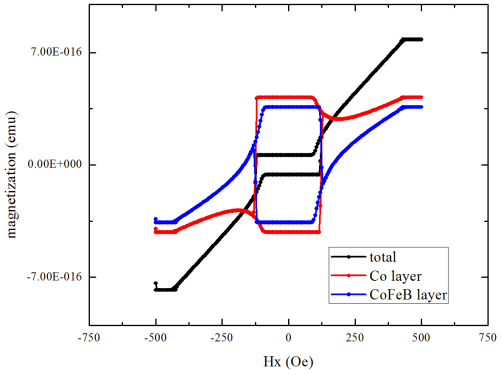

FIGURE 4.14: Simulation of two strongly coupled in-plane layers.

The obtained coupling constants can be found in table 4.1. A small difference is found between the strength of the coupling in the in-plane or in the out-of-plane case. This is probably due to different growth conditions; the base pressure in the sputtering machine varies a bit between different days, which could result in a small difference in growth rate and film quality. If the thicknesses of Ru and Pt layers are not exactly the same in the samples, the coupling will be different. Also the uncertainty in the coupling constant is non negligible, because the saturation field cannot be determined with high accuracy, though it is difficult to quantify how large this uncertainty is exactly. The values obtained here can be compared to others reported in literature [7], where, the same as here, Pt was inserted between Ru and magnetic layers to "dilute"the RKKY coupling. Those results and the ones presented here differ in a value corresponding to Pt thickness variations of 1 Ångström.

TABLE 4.1: Coupling constants for completely out-of-plane or in-plane systems.

System	J (erg/cm^2)
weakly coupled out-of-plane	0.019
weakly coupled in-plane	0.031
strongly coupled out-of-plane	0.088
strongly coupled in-plane	0.078

4.2 The search for canted states, a systematic study

Once H_J is known, the thickness of the layers is varied, one of them close to the spin reorientation transition, to achieve canted states. In table 4.2 an overview is given of the samples grown that will be discussed in the following sections.

TABLE 4.2: Overview of the samples grown in this study.

Series	t_{Co} (nm)	t_{CoFeB} (nm)	t_{Pt} (nm)	t_{Ru} (nm)
1	2.0	0.6 to 2.0	0.5	1.0
2	2.1	0.6	0.5	1.0
3	2.0	0.6 to 1.8	0.7	1.0
4	2.2	1.2 to 1.8	0.7	1.0
5	2.0	0.6	0.7	0.3 to 1.4

4.2.1 First series

For the first attempt to find canted states a series of samples is grown with 2.0 nm Co, strong coupling and varying CoFeB thickness. From section 4.1.1 it is known that a 2.0 nm Co layer has an in-plane anisotropy, but can probably easily be pulled out-of-plane because it is close to the spin reorientation transition. Polar MOKE measurements of this series are shown in figure 4.15 to 4.18.

Figure 4.15 shows the type of loop observed for CoFeB thicknesses smaller than 1.2 nm. The CoFeB has a strong out-of-plane anisotropy in this regime, and the Co is pulled out-of-plane by the coupling. When the field sweeps from negative to positive, or vice versa, three steps in the magnetization are observed. This may seem counterintuitive at first sight because there are only two magnetic layers. The CoFeB layer is much thinner than the Co layer, so according to equation 2.3 the CoFeB layer experiences a much higher coupling field. This means that when the system relaxes from, for instance negative, saturation, the CoFeB layer will be the first to switch and the system will be in an antiparallel state. When the field becomes positive the thick layer is not aligned with the field, which is unfavorable regarding the Zeeman energy. By switching to the other antiparallel state the system minimizes both Zeeman and coupling energy. For high positive fields both layers align with the field, resulting in three steps in total. This behavior is typical for ferrimagnets [13].

When the CoFeB gets thicker, the difference in Zeeman energy between the two antiparallel states becomes smaller. At a certain point it will be too small and the system will never switch from the one antiparallel state to the other. The loop now only has two steps, like in figure 4.16.

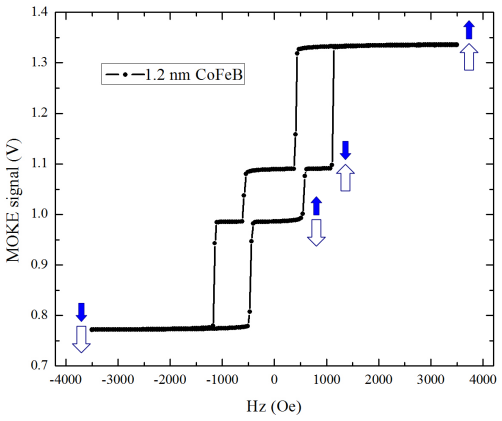

FIGURE 4.15: Polar MOKE measurement of a sample with 2.0 nm Co, 1.2 nm CoFeB and strong coupling.

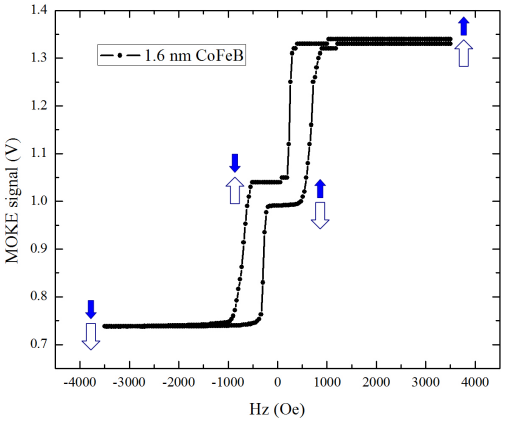

FIGURE 4.16: Polar MOKE measurement of a sample with 2.0 nm Co, 1.6 nm CoFeB and strong coupling.

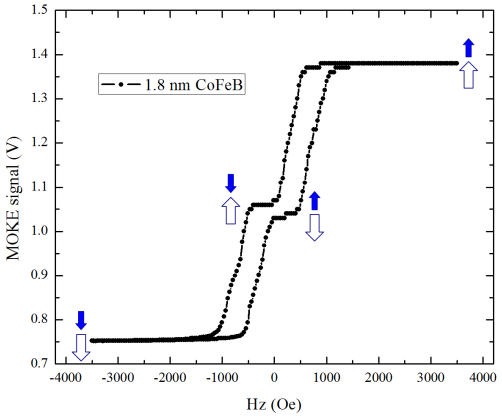

FIGURE 4.17: Polar MOKE measurement of a sample with 2.0 nm Co, 1.8 nm CoFeB and strong coupling.

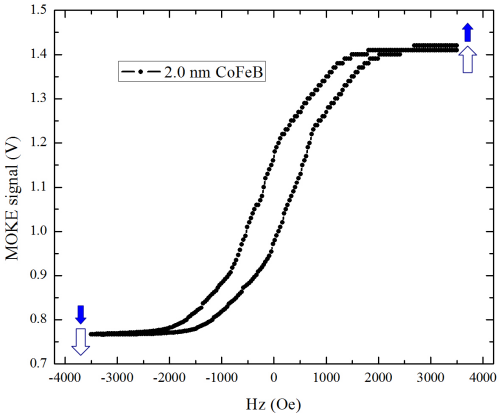

FIGURE 4.18: Polar MOKE measurement of a sample with 2.0 nm Co, 2.0 nm CoFeB and strong coupling.

When the CoFeB thickness is increased from 1.6 to 1.8 nm, the spin reorientation transition is crossed, the CoFeB is now intrinsically in-plane, although the external magnetic field can still pull the magnetization out-of-plane easily. The loop becomes much more slanted, see figure 4.17.

Ising simulations are performed to reproduce these loops, see figure 4.19 and 4.20. Note that the loop in figure 4.15 can only be reproduced by combining major and minor loops. This will be explained further in section 4.2.5. The loops shown in figure 4.17 and 4.18 clearly show non Ising behavior. These are typical examples of loops that unfortunately cannot be reproduced using the available simulation methods.

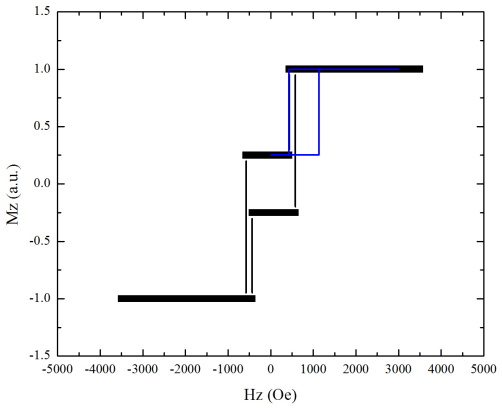

FIGURE 4.19: Simulation of a system with 2.0 nm Co, 1.2 nm CoFeB and strong coupling.

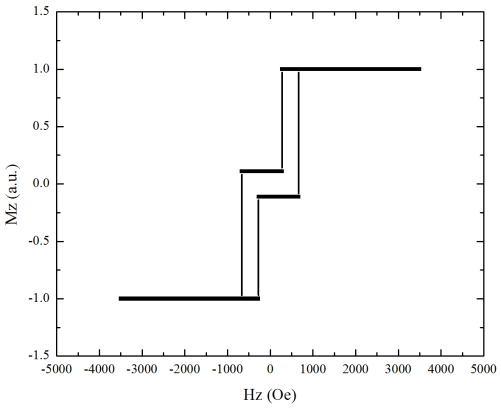

FIGURE 4.20: Simulation of a system with 2.0 nm Co, 1.6 nm CoFeB and strong coupling.

4.2.2 Second series

Next a sample is grown with 2.1 nm Co, 0.6 nm CoFeB and still strong coupling. Both out-of-plane and in-plane measurements are shown in figure 4.21 and 4.22.

These loops indicate a canted state; at remanence the magnetization of the Co layer is neither completely in-plane nor completely out-of-plane. This can be seen more clearly in the simulations. The simulations are able to reproduce the behavior of the system, compare figure 4.23 to figure 4.22. From the simulations we can extract the behavior of the individual layers during switching, this is plotted in figure 4.24. The effective anisotropy for a 0.6 nm thick CoFeB layers corresponds to a 24000 Oe field, so it was expected that the in-plane fields used during this measurement are too weak to pull the CoFeB magnetization from the out-of-plane direction. The simulations show indeed that the CoFeB layer stays fixed during the whole measurement. Simulations give the angles of the magnetization of both layers as well. At remanence the polar angle of Co is about 130 degrees instead of 0 or 90, indicating that the Co layer is in a canted state. Unfortunately, no series of similar samples with different CoFeB thicknesses were grown, but it would be advisable to do so in future projects.

4.2.3 Third series

In the first series samples with small CoFeB thicknesses showed almost perfect out-of-plane behavior. This means that the Co layer is pulled completely out-of-plane by the coupling. This series is repeated using a weaker coupling, with Pt spacers now 0.7 nm thick instead of 0.5 nm. MOKE measurements with applied fields in the z direction are shown in figure 4.25 to 4.28.

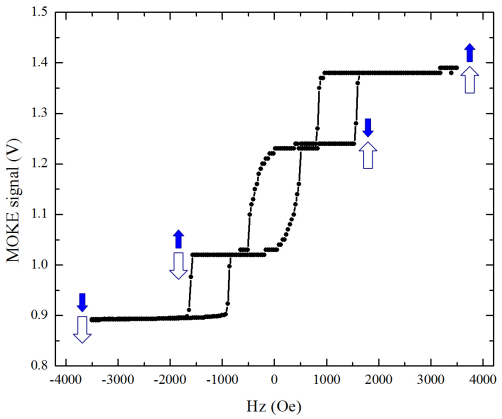

FIGURE 4.21: Polar MOKE measurement of a sample with 2.1 nm Co, 0.6 nm CoFeB and strong coupling.

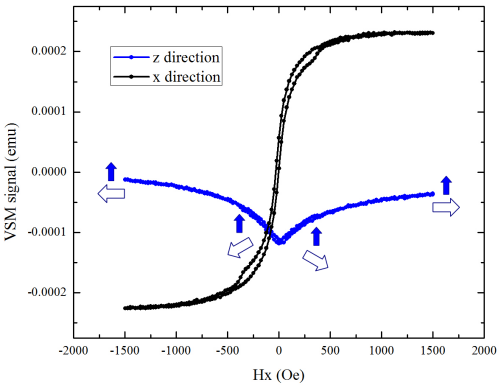

FIGURE 4.22: In-plane VSM measurement of a sample with 2.1 nm Co, 0.6 nm CoFeB and strong coupling.

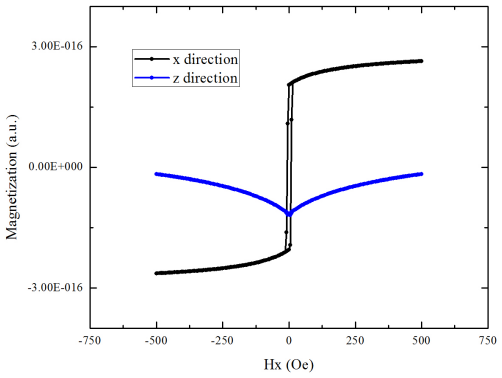

FIGURE 4.23: Simulation of the behavior of the sample with 2.1 nm Co, 0.6 nm CoFeB and strong coupling.

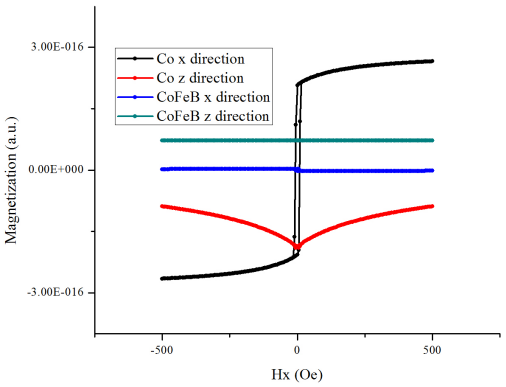

FIGURE 4.24: Magnetization of the individual layers according to the simulations.

A loop with three steps and a clearly out-of-plane behavior is found for a CoFeB thickness of 0.6 nm, as can be seen in figure 4.25. This loop resembles the one obtained in the case of strong coupling, though the transitions between parallel and anti parallel states occur at lower fields, consistent with the fact that the coupling is now lower. Only two switches occur when the CoFeB thickness is increased to 0.8 nm or more, see figure 4.26 and 4.27. Note however, that the shapes of the two step graphs in figure 4.26 and 4.27 are different from each other; in the sample with 0.8 nm CoFeB, first a small sharp switch happens, corresponding to a switch of the CoFeB layer, and after that a larger more slanted switch occurs, corresponding to a switch of the Co layer. For the sample with 1.2 nm CoFeB it is the other way around; the larger and more slanted switch happens before the small sharp one. This can be explained in the following way using the Ising approximation, see figure 4.29.

When the system relaxes from positive saturation, a layer will switch at the following field:

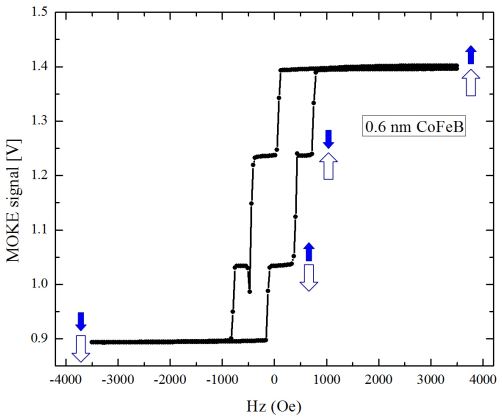

FIGURE 4.25: Polar MOKE measurement of a sample with 2.0 nm Co, 0.6 nm CoFeB and weak coupling.

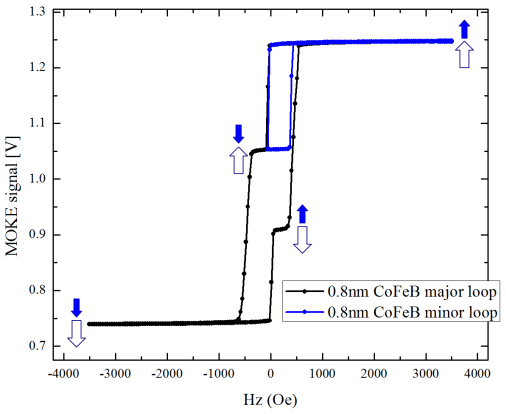

FIGURE 4.26: Polar MOKE measurement of a sample with 2.0 nm Co, 0.8 nm CoFeB and weak coupling.

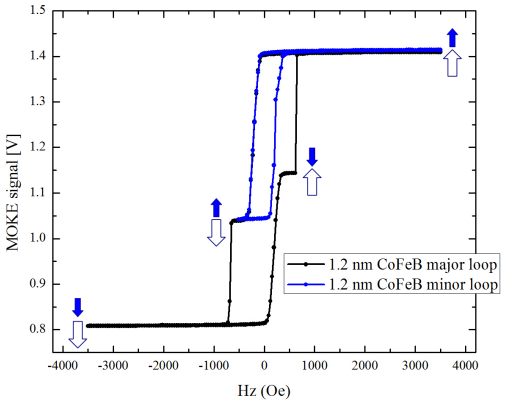

FIGURE 4.27: Polar MOKE measurement of a sample with 2.0 nm Co, 1.2 nm CoFeB and weak coupling.

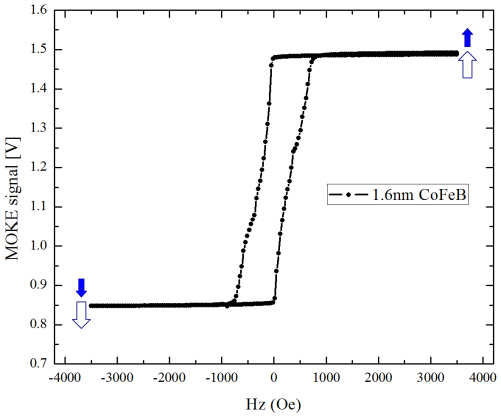

FIGURE 4.28: Polar MOKE measurement of a sample with 2.0 nm Co, 1.6 nm CoFeB and weak coupling.

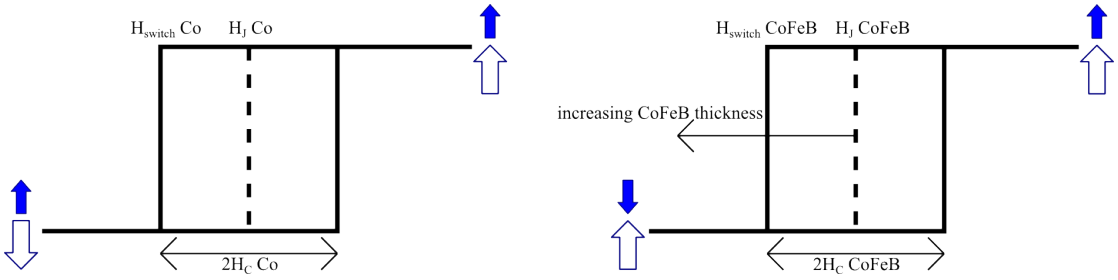

FIGURE 4.29: Schematic explanation of why which layer switches first depends on the CoFeB thickness.

$$H_{switch} = H_J - H_C \tag{4.1}$$

In this equation H_C is the coercive field and H_J the coupling field. The equation holds for both the Co and the CoFeB layer. If H_{switch} is higher for the Co layer, then this field

will be reached before H_{switch} for CoFeB when the system relaxes from saturation, and the Co layer switches first. If H_{switch} is higher for the CoFeB layer, it is the other way around. In this series the Co thickness is constant, so H_{switch} is constant for this layer. The CoFeB thickness is varied. The coercive field can depend on the layer thickness, but in the regime where the transition between the two switching orders takes place H_C is approximately constant. The coupling field depends on the thickness as described in equation 2.3. This means that for the CoFeB layer H_J, and therefore H_{switch}, is larger for thin layers and smaller for thick layers. So for systems with a thin CoFeB layer, the CoFeB layer should switch first and for systems with a thick CoFeB layer the Co layer should switch first, which is in agreement with the measurement results. A sample with 1.0 nm CoFeB was grown in this series as well, which turned out to be exactly on the transition between these two switching possibilities. This is further discussed in chapter 4.4.

These samples were also measured using VSM with fields applied in the x direction. The results for the 0.8 nm CoFeB sample are shown in figure 4.30 and 4.31. In figure 4.30 a saturating positive z field was applied before the measurements were conducted, while in figure 4.31 a saturating negative z field was applied.

The fields that are used are not strong enough to pull the CoFeB layer in-plane, since it has a strong out-of-plane anisotropy. Therefore its magnetization stays in the z direction, positive or negative depending on the direction of the saturation field that was applied before the measurement, throughout the entire measurement. The Co layer is close to the spin reorientation transition and can follow the applied field more easily; when the applied x field is negative (positive) its magnetization points in the negative (positive) x direction. At low x fields its magnetization will be antiparallel to the CoFeB layer because of the coupling. The small hysteresis observed can be caused by domains or canting. This all explains the butterfly shape observed in the z component of the measured magnetization. Simulations of these systems are shown in figure 4.32 and 4.33. There are some discrepancies between experiments and simulations; the x direction loop in the experiments has a much larger hysteresis and is more slanted (notice the numbers on the x axes). Also the butterfly shape in the z direction loop is more rounded in the experiments. It is also possible to set the parameters in such a way that a rounded loop is simulated, but then the hysteresis disappears (these loops are not shown here). The next step to improve the simulations will be adding a second order anisotropy constant, as introduced in section 2.3.1. Because the Co layer has a thickness close to the spin reorientation transition this second order term becomes important and could change the results of the simulations. Another explanation for the discrepancies would be that the macrospin approximation is invalid for these samples; the effect of domains could affect the shape of the loops, explaining the discrepancies stated.

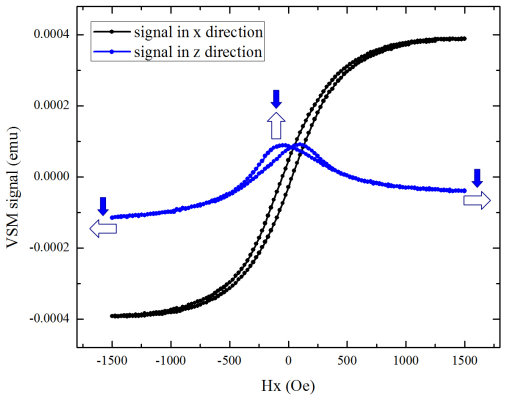

FIGURE 4.30: In-plane VSM measurement of a sample with 2.0 nm Co, 0.8 nm CoFeB and weak coupling, after a positive saturating z field was applied.

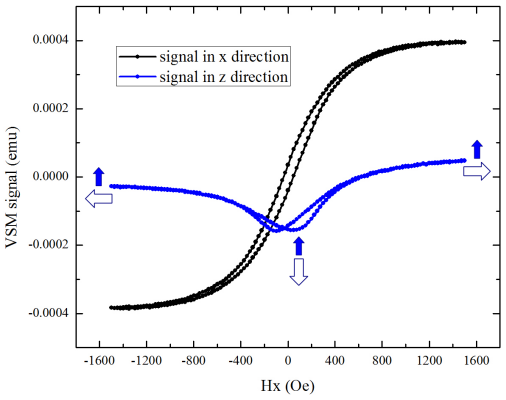

FIGURE 4.31: In-plane VSM measurement of a sample with 2.0 nm Co, 0.8 nm CoFeB and weak coupling, after a negative saturating z field was applied.

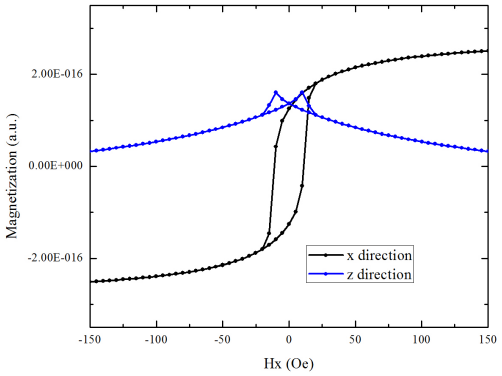

FIGURE 4.32: In-plane VSM measurement of a sample with 2.0 nm Co, 0.8 nm CoFeB and weak coupling, after a positive saturating z field was applied.

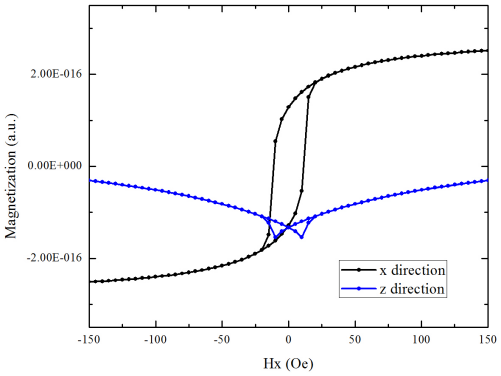

FIGURE 4.33: In-plane VSM measurement of a sample with 2.0 nm Co, 0.8 nm CoFeB and weak coupling, after a negative saturating z field was applied.

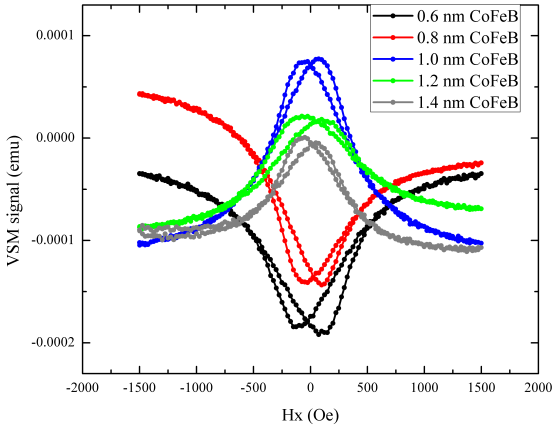

FIGURE 4.34: Butterfly loops for samples with different CoFeB thicknesses after a negative z saturation field was applied.

The z components of the magnetization while x fields are applied are shown in figure 4.34. for all samples of this series, except for the samples with 1.6 nm CoFeB or more,

because these samples are fully in-plane. The amplitude of the butterflies decreases when the thickness of the CoFeB layer increases. This is because the out-of-plane anisotropy of the CoFeB layer decreases when it becomes thicker. So for the thicker CoFeB samples the Co magnetization is not in-plane at zero field, but also not completely out-of-plane, which would mean it is a canted state. Again, we must be carefull with this conclusion since the simulations are not reproducing the experiments perfectly and the hysteresis could be associated with domains in the sample.

The butterflies in figure 4.34 are not all in the same direction, though the same z saturation field was applied before the measurement in all these cases. This has to do with a phenomenon described earlier in this paragraph; after the saturating z field is applied the system relaxes. But which of the two layers now switches depends on the thickness of the CoFeB, as was previously shown in the out-of-plane MOKE measurements. So the final direction of the CoFeB magnetization, and therefore the direction of the butterfly, depends on the thickness of the CoFeB layer.

4.2.4 Fourth series

At least one canted state has been produced. However, the loops in figures 4.21 and 4.25 to 4.27 resemble those found for completely out-of-plane systems. In the next series a canted state closer to perfectly in-plane situation is pursued. To do this, samples with 2.2 nm Co layers are grown, which should provide a stronger in-plane anisotropy than the 2.0 nm layers that were used in the previous series (2.0 nm Co has a K_{eff} corresponding to an effective field of -450 Oe and 2.2 nm Co has a K_{eff} corresponding to an effective field of -2000 Oe). The Pt spacers are 0.7 nm thick, corresponding to weak coupling.

The samples are more in-plane indeed, when fields are applied in the x direction, hardly any change in the z component is detected (not shown here). The VSM results when a z field is applied are shown in figure 4.35 to 4.38.

The two layers behave independently for the sample with 1.2 nm thick CoFeB, shown in figure 4.35. This is because the CoFeB layer is strongly out-of-plane while the Co layer is strongly in-plane. The sloped part of the graph represents the in-plane Co layer that is pulled out-of-plane by the applied field, the sharp switches represent the CoFeB layer. In the x direction the x component of the Co magnetization is measured, but note that it can have a significant y component as well that cannot be measured.

The sample with 1.8 nm CoFeB has no sharp switch at all; both layers are in-plane, so the result is a hard axis loop.

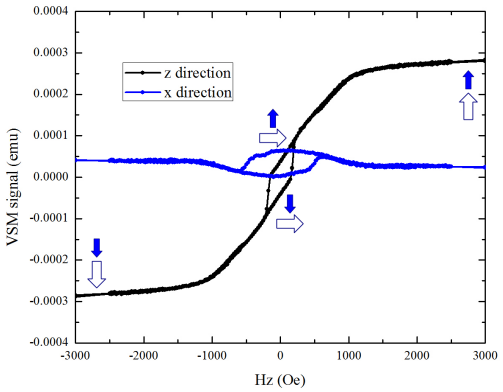

FIGURE 4.35: Out-of-plane VSM measurement of a sample with 2.2 nm Co, 1.2 nm CoFeB and weak coupling.

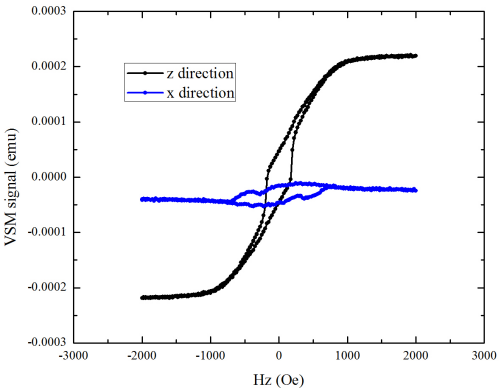

FIGURE 4.36: Out-of-plane VSM measurement of a sample with 2.2 nm Co, 1.4 nm CoFeB and weak coupling.

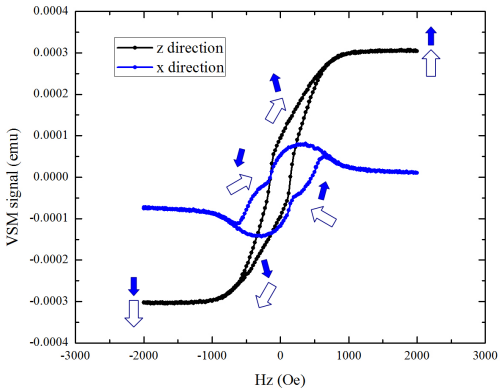

FIGURE 4.37: Out-of-plane VSM measurement of a sample with 2.2 nm Co, 1.6 nm CoFeB and weak coupling.

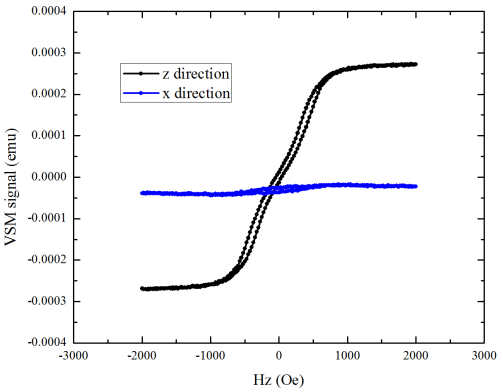

FIGURE 4.38: Out-of-plane VSM measurement of a sample with 2.2 nm Co, 1.8 nm CoFeB and weak coupling.

The samples with 1.4 and 1.6 nm CoFeB on the contrary, show a wide variety of interesting features, and simulations are necessary to understand them. The loops could be reproduced qualitatively by the simulations, see figure 4.39. This gives all the information necessary to deduce the behavior of the individual layers. The Co layer turns out to behave almost like a normal in-plane layer; The magnetization is almost in-plane at remanence being canted 4 degrees and can, be pulled out-of-plane by the magnetic field, resulting in a hard axis loop. The CoFeB layer has intrinsically an out-of-plane magnetization but is close to the spin reorientation transition. At remanence it is in a canted state due to the coupling, being canted 13 degrees according to simulations. The simulations also explain the strange kinks in the loop, in figure 4.39 this is schematically depicted next to the loops.

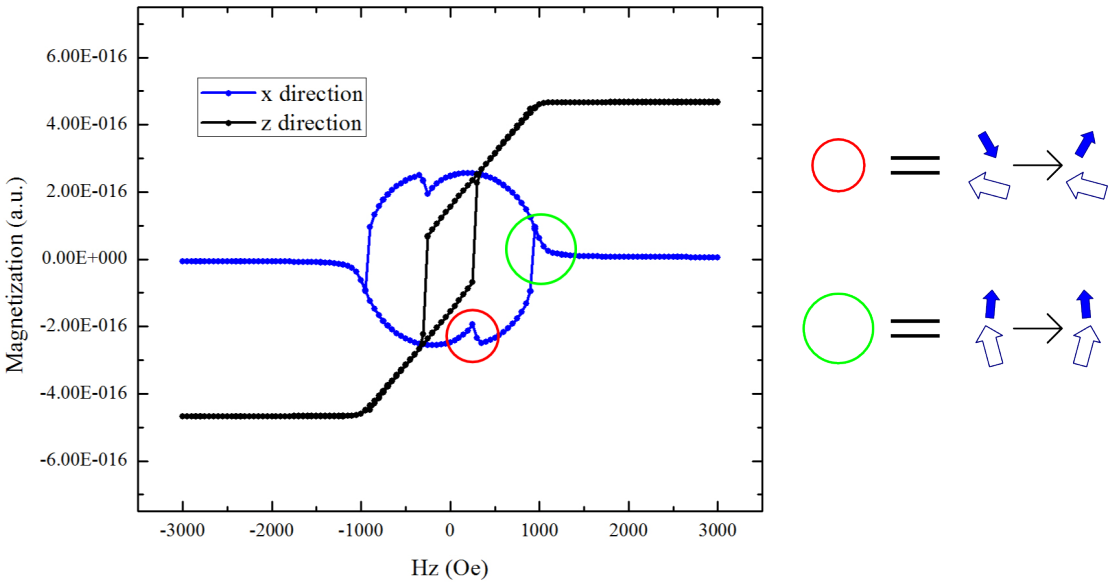

FIGURE 4.39: Simulation of the sample with 2.2 nm Co, 1.6 nm CoFeB and weak coupling.

4.2.5 Fifth series

To complete this systematic study, a series is grown for which the Ru thickness is varied. This changes the coupling, not only in strength, but it can become ferromagnetic instead of anti-ferromagnetic, as all the cases studied before. The parameters that are used are: 2.0 nm Co, 0.6 nm CoFeB and weak coupling. These parameters resulted in the butterfly shape discussed before.

In series 1 to 4 the Ru layer is always 1.0 nm thick, so the sample with 1.0 nm Ru in this series should give the same results as the sample with 0.6 nm CoFeB in the third series. The results are similar indeed, compare figure 4.40 to 4.25. A 1.4 nm thick Ru layer results in ferromagnetic coupling. When this type of coupling is strong enough, an antiparallel state is not stable. This is why both layers switch at the same time, resulting in a graph with only one step, figure 4.41.

As observed in figures 4.42 and 4.43, the butterfly shape of the z component of the magnetization under applied x fields exists for both anti-ferromagnetic and ferromagnetic coupling. In general we observe that the hysteresis in the parabola becomes clearer when the coupling is weak and disappear when the coupling becomes strong. In both ferromagnetic and anti-ferromagnetic case after saturating the sample in the same direction, the butterfly shape (magnetization of Co) point in the same direction after saturation in the same direction, which may seem counter intuitive. This can be explained in the following way. Only the Co layer changes its magnetization when x fields are applied to these samples, the CoFeB layer stays fixed in the z direction, as explained in section

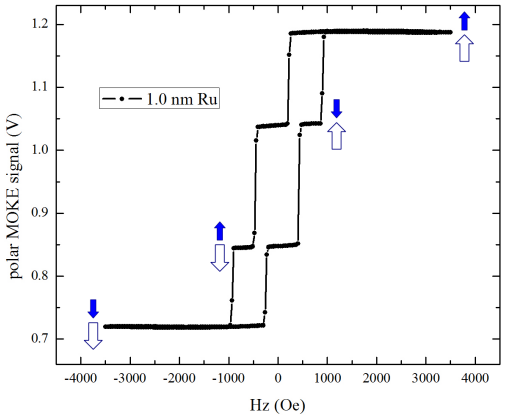

FIGURE 4.40: Polar MOKE measurement of a sample with 2.0 nm Co and 0.6 nm CoFeB and anti-ferromagnetic coupling.

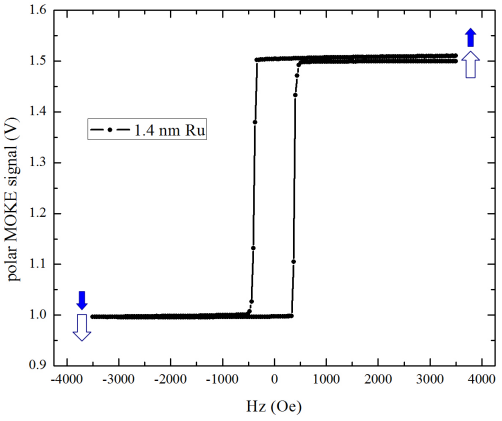

FIGURE 4.41: Polar MOKE measurement of a sample with 2.0 nm Co and 0.6 nm CoFeB and ferro-magnetic coupling.

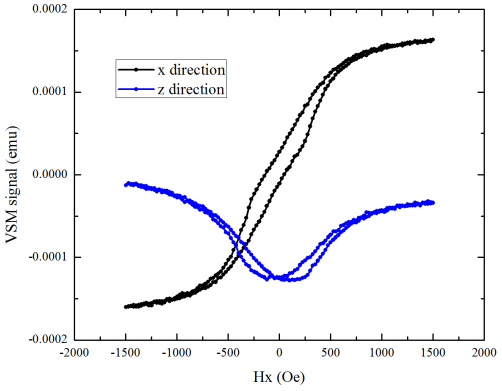

FIGURE 4.42: In-plane VSM measurement of a sample with 2.0 nm Co and 0.6 nm CoFeB and anti-ferromagnetic coupling.

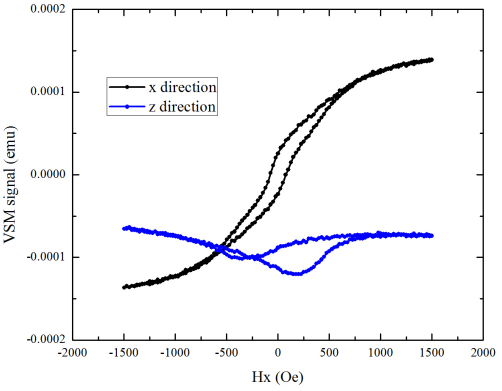

FIGURE 4.43: In-plane VSM measurement of a sample with 2.0 nm Co and 0.6 nm CoFeB and ferro-magnetic coupling.

4.2.3. Whether the CoFeB layer is fixed in the positive or negative z direction depends on the saturation before the actual measurements. After saturating the sample in the positive z direction and relaxing the field, CoFeB points in the positive z direction in the ferromagnetic case, but in the negative direction in the anti-ferromagnetic case, because the system switches to the other anti-parallel state. This is schematically summarized in figure 4.44. This means that the Co layer will have its magnetization in the positive z direction in both the ferromagnetic and anti-ferromagnetic case, so the butterflies should have the same shape for both couplings!

The polar MOKE loops in this section are successfully reproduced by Ising simulations. Only some of the loops with three steps show problems, as encountered before in section 4.2.1. In figure 4.46 the result of a MOKE measurement is shown and in the inset the corresponding simulations are shown. The measurement shows a loop with three steps, but the simulation shows a loop with only two steps. It is not fundamentally impossible

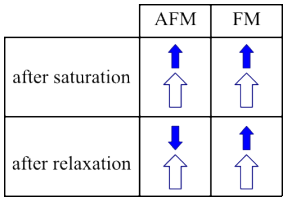

FIGURE 4.44: Schematic explanation of why which layer switches first depends on the CoFeB thickness.

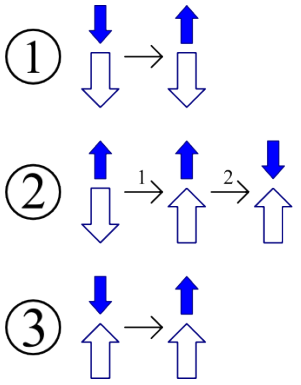

FIGURE 4.45: Measurement after saturation with a negative z field.

for Ising simulations to produce loops with three steps, see for example figure 4.47. So how can this discrepancy between simulation and experiment be explained? In figure 4.46 and 4.47 the transitions are numbered and in figure 4.45 the interpretation according to simulation of these transitions are given. Transition 2 has to happen in two steps because in the simulation only one layer can switch at a time. The switching fields for these transitions are:

$$1)\ H_{switch} = H_{CCoFeB} - \frac{J}{t_{CoFeB}} \tag{4.2}$$

$$2.1)\ H_{switch} = H_{CCo} + \frac{J}{t_{Co}} \tag{4.3}$$

$$2.2)\ H_{switch} = -H_{CCoFeB} + \frac{J}{t_{CoFeB}} \tag{4.4}$$

$$3)\ H_{switch} = H_{CCoFeB} + \frac{J}{t_{CoFeB}} \tag{4.5}$$

Note that transition 1 and 2.2 are the same except for a minus sign. A loop with three steps is only obtained in simulations if transition 2.2 can follow after 2.1. This only happens when the switching field of 2.1 is larger than the switching field of 2.2. So "open" loops, see the blue circle in figure 4.46, cannot be simulated with the used program, while "closed" loops, see the blue circle in figure 4.47 can. The fact that open loops do occur in reality indicates that both layers have to switch at the same time when going from the one anti-parallel state to the other, which is not possible in the Ising simultions.

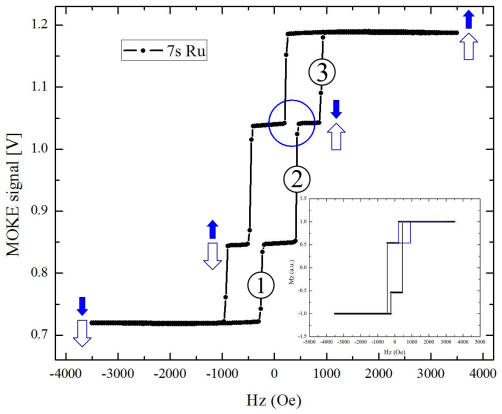

FIGURE 4.46: Example of a "open" loop measured in the polar MOKE. Inset shows the corresponding loop produced by simulations.

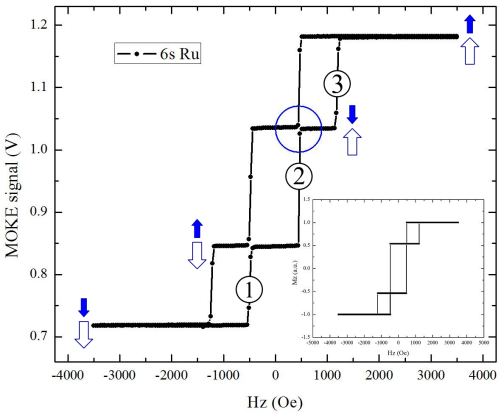

FIGURE 4.47: Example of a "closed" loop measured in the polar MOKE, Inset shows the corresponding loop produced by simulations.

The coupling strength can be calculated from measured loops in case of anti-ferromagnetic coupling. The loops have been reproduced using Ising simulations. The coupling strength can also be inferred from the parameters that are set to reproduce the loops, also for the ferromagnetic case. The results are shown in figure 4.48 being in agreement with the RKKY expected dependence and other results found in literature [14].

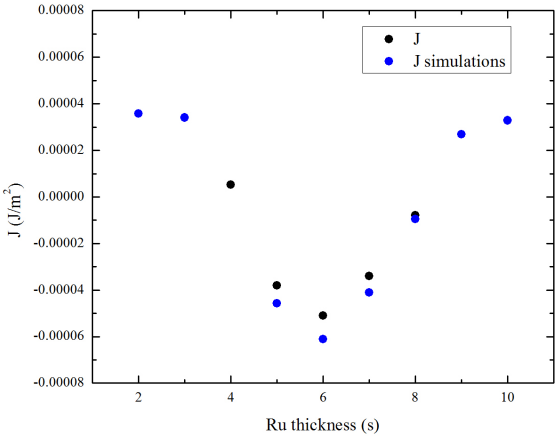

FIGURE 4.48: Coupling strength as a function of the ruthenium thickness.

4.3 Analysis of the bias

In some of the samples studied in the second and fourth series a small bias is observed during measurements with x fields, its sign depending on the previous saturation with z fields. If these systems are going to be used for the injection of multiple solitons, it is essential that a bias is created. That is why this effect is studied in more detail in this section. An example of a sample that showed a bias, 2.0 nm Co 1.2 nm CoFeB and weak

coupling, is shown in figure 4.49 and 4.50. This effect is small, but it has been observed more clearly in CoFeB-CoFeB systems, see figure 4.51 and 4.52.

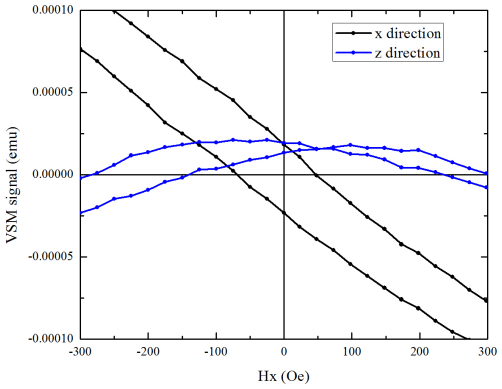

FIGURE 4.49: Measurement after saturation with a positive z field.

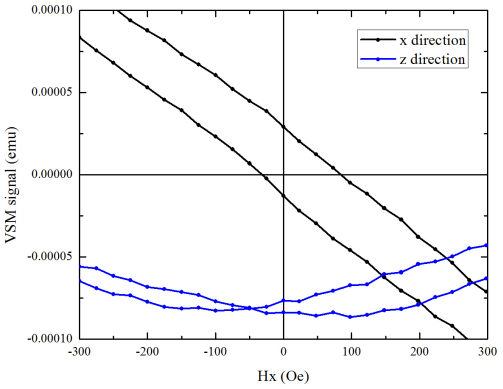

FIGURE 4.50: Measurement after saturation with a negative z field.

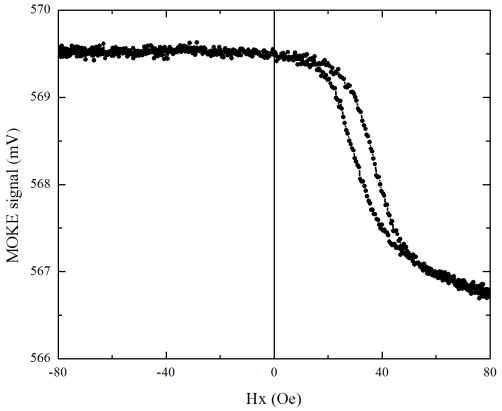

FIGURE 4.51: Measurement of a CoFeB-CoFeB sample after saturation with a positive z field (measured by Dr. A. Fernández-Pacheco).

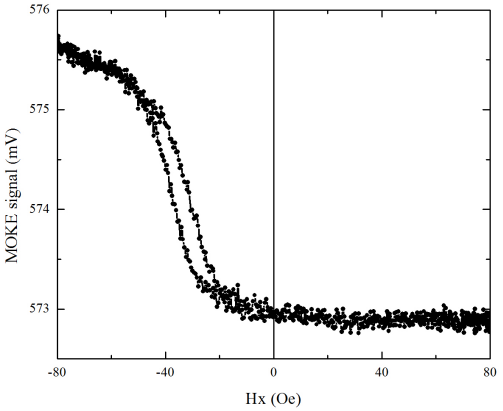

FIGURE 4.52: Measurement of a CoFeB-CoFeB sample after saturation with a negative z field (measured by Dr. A. Fernández-Pacheco).

A small shift in the loops is visible. In the second series the bias seems to vary randomly with the CoFeB thickness; sometimes it is large other times small, sometimes it is positive other times negative. A possible explanation could be that the easy axes of the in-plane and out-of-plane layer are not orthogonal.If this was the case, this indeed induces a bias [15]. This would explain why the dependence on the CoFeB thickness appears so random, because the bias would depend on the in-plane angle under which the sample was mounted into the VSM. It would also explain why a bias can exist at all, since an effect breaking the symmetry of the system is necessary to produce this kind of effect. Two contributions could cause non-orthogonal easy axes: one possible explanation would be that the silicon substrate was not perfectly flat, but has atomic steps since it was miscut, see figure 4.53 The Co layer is thick and has an in-plane (shape)anisotropy. The easy axis would be perpendicular to the surface normal, which is not necessarily equal to the crystallographic Si(001) plane. A second contribution could be the following; the

thin CoFeB layer has an out-of-plane anisotropy with the easy axis direction parallel to the Pt(111)direction, which might be not perfectly aligned with the Si(001) direction due to structure forming during the growth. It is also schematically pictured how this non-orthogonality could induce a bias. Simulations confirm that a bias indeed occurs when the easy axes are not perpendicular.

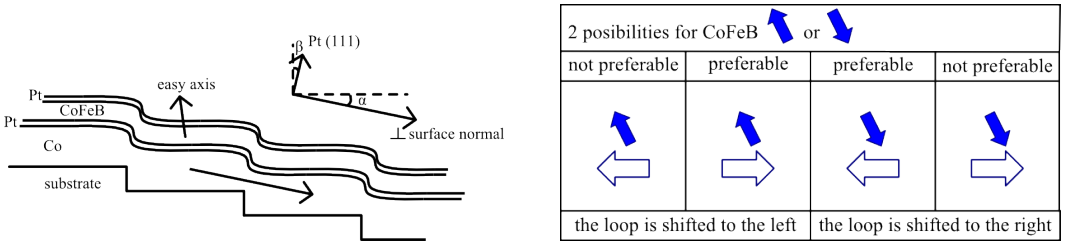

FIGURE 4.53: Schematic explanation of how a miscut can cause non orthogonal easy axes, and how non orthogonal easy axes can induce a bias.

.

To test this theory, the following experiment is conducted: the bias field of a sample, 2.0 nm Co 0.6 nm CoFeB and weak coupling, is measured using MOKE for different angles under which the sample is mounted, see figure 4.54. The observed (in-plane) angular dependence is in agreement with the theory presented before, but to be certain additional experiments are necessary. X-ray reflection could show the orientation of the surface normal and X-ray diffraction could show the orientation of the Si(001) and Pt(111) crystallographic planes. This data was unfortunately not yet available at the time this report was written.

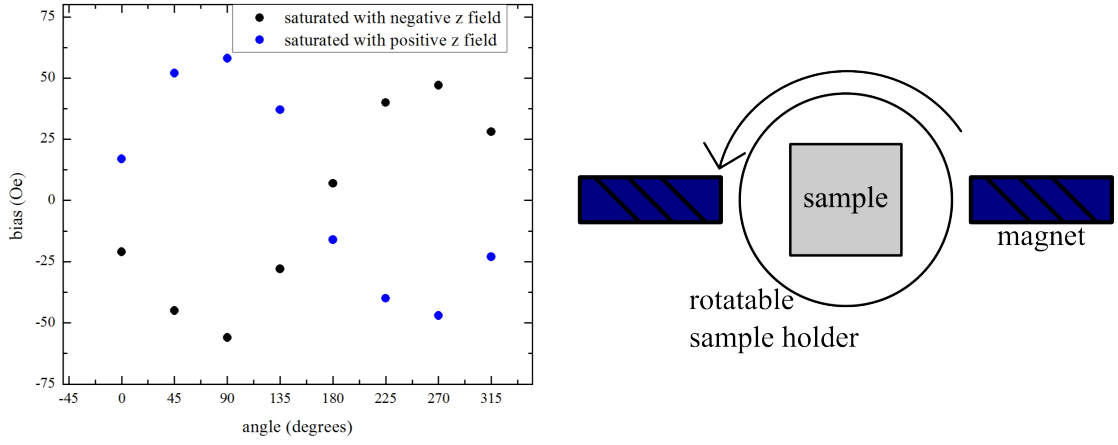

FIGURE 4.54: Bias as a function of the angle under which the sample is mounted in the MOKE.

4.4 Two switching possibilities

In section 4.2.3 it was explained whether the CoFeB or Co layer switches first depending on on the thickness. One of the samples in this series turned out to be exactly on at the crossover between those two possibilities: the one with 2.0 nm Co, 1.0 nm CoFeB and weak coupling. In this section this sample is further investigated.

Which layer switches first turns out to depend on the rate of the sweeping field. Figure 4.55 and 4.56 show MOKE measurements of the same spot on the sample, the only difference is the sweeping rate. The sharp switch corresponds to the CoFeB layer, the slanted switch to the Co layer.

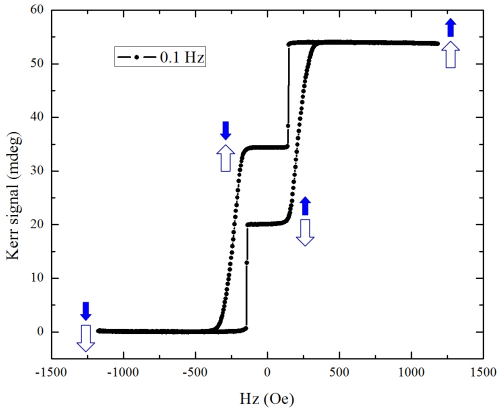

FIGURE 4.55: Measurement at a low rate, 400 Oe/s.

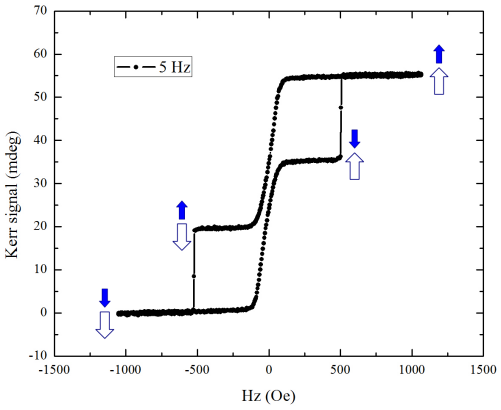

FIGURE 4.56: Measurement at a high rate, 20000 Oe/s.

It turns out that a large range of rates exist for which both switching orders are possible. Sometimes both possibilities even occur in the same loop, see the inset of figure 4.57. Some statics are shown in figure 4.57. Ten loops are measured at every rate, and the number of times that the CoFeB switches first is counted. This way a probability can be calculated.

When the system relaxes from saturation, the first switch occurs at $H_J - H_C$. If this field is higher for CoFeB, the CoFeB layer switches first, if this field is higher for Co the Co layer switches first. It is well known that the coercive field of a single layer is dependent on the sweep rate [16]. We indeed find this is measurements on the single layer samples previously shown in section 4.1.1, see figure 4.58 For thin samples the frequency dependence is much stronger than for thick samples. This difference is because thin and thick samples switch using a different mechanism. This could be seen in the images shown in figures 4.5 to 4.8. Thin samples switch with big domain and are dominated by the motion of domain walls. Samples with a thickness close to the spin reorientation transition switch with many small domains and are nucleation dominated. The bilayer investigated in this section consists of a thin CoFeB layer which switches

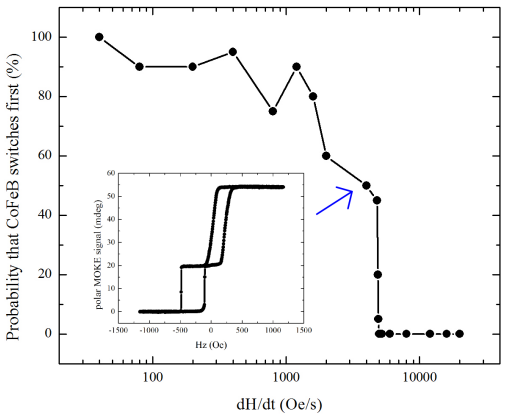

FIGURE 4.57: Probability that CoFeB switches first vs sweep rate. Inset shows a loop with a different switching order when going up and down.

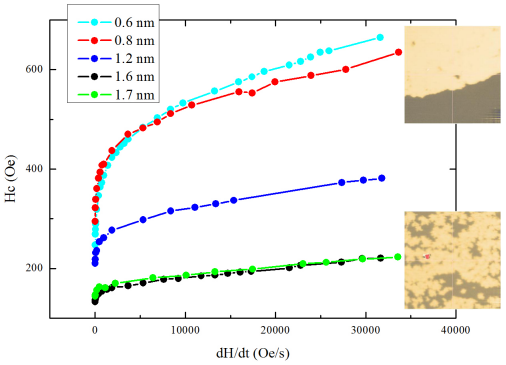

FIGURE 4.58: Dependence of the coercive field on the sweep rate for single layers with different thicknesses, measured by Dr. A. Fernández-Pacheco. Images show domains during the switch of a thin and a thick layer.

with big domains and a thick Co layer which switches with small domains, see figure 4.59. Because of this difference the dependence on the sweep rate is different for the two layers and it is indeed possible to find a change in the order of switching at a certain sweep rate.

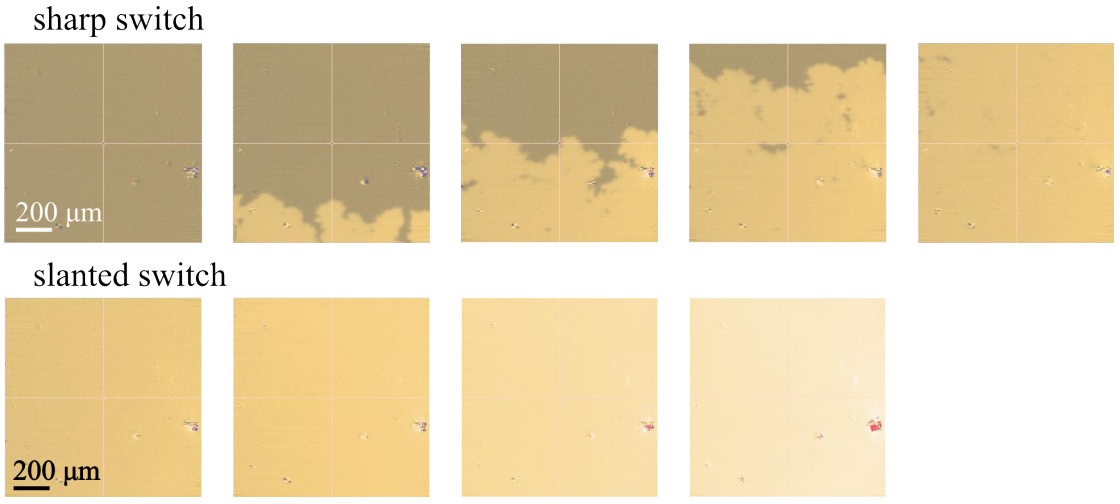

FIGURE 4.59: Polar MOKE images of two switches in a bilayer sample with 1.0 nm CoFeB and 2.0 nm Co.

Chapter 5

Conclusion

Anti-ferromagnetically coupled bilayer Cobalt-CoFeB systems have been investigated systematically to create canted states of the magnetization. A system with a 0.6 nm CoFeB layer and 2.1 nm Co layer strongly coupled results in a canted state; the CoFeB stays out of plain but the Co becomes canted 40 degrees from the in-plane situation according to simulations. A system with a canted CoFeB layer was created as well; 1.6 nm CoFeB, 2.1 nm Co weakly coupled. In this case the Co is 4 degrees from the in-plane situation and the CoFeB is canted 13 degrees from the out-of-plane situation. A next step in this research could be the investigation of trilayer systems.

A bias was observed in some of the investigated systems. A possible explanation for this effect is the existence of non-orthogonal easy axes of the out-of-plane and in-plane layer. X-ray diffraction measurements are in progress. The presence of a bias field is interesting for applications. It could be increased by using a substrate with an intentional larger miscut.

One of the grown samples turned out to have a switching mechanism dependent on the sweep rate of the magnetic field. The different frequency dependence of the coercivity for both layers, due to the different switching mechanisms they present, together with the different coupling field for both layers is responsible of this interesting behavior.

Chapter 6

Acknowledgements

This internship has been a great experience for me, and I would like to thank the people who have made this possible. First of all I would like to thank Henk Swagten and Reinoud Lavrijssen from my home university, Eindhoven University of Technology. They had the contacts to make this possible and I would like to thank them for their trust in letting me represent our university in such a prestigious place as Cambridge. Next I would like to thank Amalio Fernández-Pacheco who has been my daily supervisor for three months. This has been a time taking job but he did it in such a positive way and I learned a lot from him. Last I would like to thank the all the members of the thin film magnetism group at the Cavendish laboratory. Everyone has been really friendly and helpful and made me feel like I was really part of group. So my thanks to Russell, Dot, Rhodri, Elle, Anthony, Dishant, Jason, Julie, Tarun, Spencer, Pete and Alex.

Bibliography

[1] R. Sbiaa, R. Law, E.L. Tan, and T. Liew. Spin transfer switching enhancement in perpendicular anisotropy magnetic tunnel junctions with a canted in-plane spin polarizer. *Journal of Applied Physics*, 105(013910), 2009. doi: 10.1063/1.3055373.

[2] C.Y. You. Reduced spin transfer torque switching current density with non-collinear polarizer layer magnetization in magnetic multilayer systems. *Apllied Physics Letters*, 100(252413), 2012. doi: 10.1063/1.4730376.

[3] R. Lavrijsen, J.H. Lee, A. Fernández-Pacheco, D.C.M.C. Petit, R. Mansell, and R.P. Cowburn. Magnetic ratchet for three-dimensional spintronic memory and logic. *Nature*, 493:647–650, January 2013. doi: 10.1038/nature11733.

[4] C. Won, Y.Z. Wu, W. Zhao, A. Scholl, A. Coran, and Z.Q. Qui. Effect of the interlayer coupling on the ni spin reorientation in ni/fe/co/cu(100). *Physical Review B*, 68(052404), 2003. doi: 10.1103/PhysRevB.68.052404.

[5] W. Kuch, Xingyu Gao, and J. Kirschner. Competition between in-plane and out-of-plane magnetization in exchange-coupled magnetic films. *Physical Review B*, 65 (064406), 2002. doi: 10.1103/PhysRevB.65.064406.

[6] J. Choi, B.-C. Min, J.-Y. Kim, B.-G. Park, J. H. Park, Y.S. Lee, and K.-H. Shin. Non-collinear magnetization configuration in interlayer exchange coupled magnetic thin films. *Applied Physics Letters*, 99(102503), 2011. doi: 10.1063/1.3634027.

[7] R. Lavrijsen, A. Fernández-Pacheco, D. Petit, R. Mansell, J.H. Lee, and R.P. Cowburn. Tuning the interlayer exchange coupling between single perpendicularly magnetized cofeb layers. *Applied Physics Letters*, 100:052411, January 2012. doi: 10.1063/1.3682103.

[8] R.L. Stamps, L. Louail, M. Hehn, M. Gester, and K. Ounadjela. Anisotropie, cone states, and stripe domains in co/pt multilayers. *Journal of Applied Physics*, 81(8), 1997. doi: 10.1063/1.365452.

[9] P. Bruno and C. Chappert. Ruderman-kittel theory of oscillatory interlayer exchange coupling. *Physical Review B*, 46(1):261–270, July 1992.

[10] M. Kisielewski, A. Maziewski, M. Tekielak, J. Ferr, S. Lemerle, V. Mathet, and C. Chappert. Magnetic anisotropy and magnetization reversal processes in pt/co/pt films. *Journal of Magnetism and Magnetic Materials*, 260:231–243, March 2003.

[11] E.Y. Vedmedenko, H.P. Oepen, and J. Kirschner. Magnetic microstructure of the spin reorientation transition. *Journal of Applied Physics*, 89(11):7145–7146, June 2001. doi: 10.1063/1.1357154.

[12] J. Ferre, J.P. Jamet, J. Pommier, P. Beauvillain, C. Chappert, R. Megy, and P. Veillet. Domains and magnetization reversal dynamics in au/co/au (111) ultrathin films: Co and au thickness dependence. *Journal of Magnetism and Magnetic Materials*, 174:77–88, 1997.

[13] N. Wiese. *Coupling phenomena and scalability of CoFeB/Ru/CoFeB sandwiches.* PhD thesis, Bielefeld University, 2006.

[14] J. Zhao, Y.J. Wang, Y.Z. Liu, X.F. Han, and Z. Zhang. Perpendicular anisotropy dependence of oscillatory interlayer coupling behavior in [pt/co]5/ru/co/[pt]5 multilayers. *Journal of Applied Physics*, 104, 2008. doi: 10.1063/1.2959378.

[15] C. Won, Y.Z. Wu, E. Arenholz, J. Choi, J. Wu, and Z.Q. Qui. Symmetry-breaking induced exchange bias in ferromagnetic ni-cu-co and ni-fe-co sandwiches grown on a vicinal cu 001 surface. *Physical Review Letters*, 99(077203), August 2007. doi: 10.1103/PhysRevLett.99.077203.

[16] B. Raquet, R. Mamy, and J.C. Ousset. Magnetization reversal dynamics in ultrathin magnetic layers. *Physical Review B*, 54(6):4128–4136, 1996.